Mechanically Powered Transparent Flexible Charge-Generating Nanodevices with Piezoelectric ZnO Nanorods

By *Min-Yeol Choi, Dukhyun Choi, Mi-Jin Jin, Insoo Kim, Sang-Hyeob Kim, Jae-Young Choi,* Sang Yoon Lee, Jong Min Kim,* and *Sang-Woo Kim**

Nanopiezotronics is an emerging area of nanotechnology with a variety of applications that include piezoelectric field-effect transistors and diodes, self-powered nanogenerators and biosystems, and wireless nano/biosensors.[1–4] By exploiting coupled piezoelectric and semiconducting characteristics, it is possible for nanowires, nanobelts, or nanorods to generate rectifying current and potential under external mechanical energies, such as body movement (handling, winding, pushing, and bending) and muscle stretching, vibrations (acoustic and ultrasonic waves), and hydraulic forces (body fluid and blood flow).[3,5–8] 1D ZnO and CdS nanostructures have been extensively investigated as a step toward realizing such self-powered energy-harvesting nanosystems and piezoelectric sensor devices.[1–10] ZnO has attracted great interest for use in electromechanical, optical, and biological devices as a result of its versatile characteristics, such as piezoelectricity, transparency, biocompatibility, low temperature, and large-area fabrication.[1–4,11–13]

It is important to detect simultaneously all forces, pressures, and vibrations in electromechanical systems, especially artificial skins or touch sensors. Flexibility and transparency are also significant in such systems in electrical-device applications, such as full touch screens and reformable displays. Most previous nanogenerators have been fabricated with nonflexible substrates, such as GaN or sapphire, for the growth of nanowires[1,14] and with nonflexible corrugated top electrodes,[1] and few studies on fully integrated flexible nanogenerators have been reported.[6,15] Also, transparent current-generating systems have not yet been created. In this work, we report the creation of fully integrated ZnO 1D nanostructure-based piezoelectric charge-generating devices suitable for use as transparent, flexible (TF) self-powered pressure sensors, which are driven by mechanical forces without any electrical sources.

ZnO nanorods on a flexible plastic substrate were prepared using an aqueous solution method (see Supporting Information, Fig. S1). This method has the advantages of simplicity, low growth temperature, large-scale growth, and mass productivity. As top electrode materials, palladium gold (PdAu) and indium tin oxide (ITO) on flexible substrates are used on the ZnO nanorods. We successfully prepared fully integrated TF current-generating devices with density-controlled ZnO nanorod arrays (over 90% transparency) and an ITO top electrode. We investigated the dependence of the output current of the nanodevices on external forces as well as on the morphologies and work functions of the top electrodes. A TF nanodevice with size $3\,\mathrm{cm} \times 3\,\mathrm{cm}$ was demonstrated to generate an output current density of about $1\,\mu\mathrm{A\,cm^{-2}}$ at a load of 0.9 kgf.

Figure 1a shows a schematic diagram of an integrated TF current generator with piezoelectric ZnO nanorods and a field-emission scanning electron microscopy (FE-SEM) image of ZnO-nanorod arrays grown on a flexible ITO-coated polyether

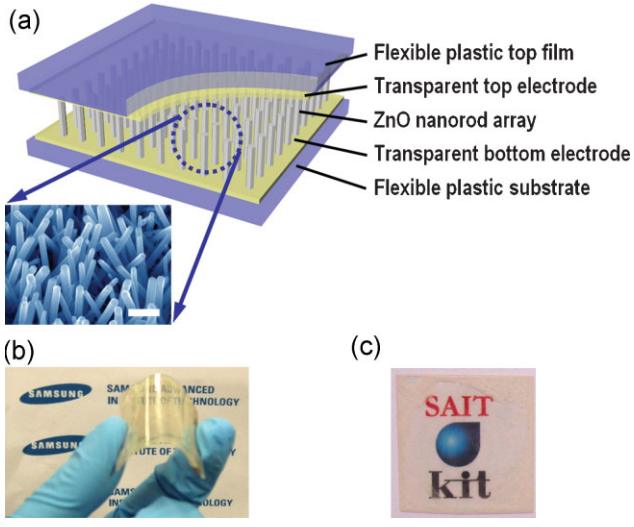

Figure 1. Fully TF charge-generating piezoelectric nanodevices with ZnO nanorods. a) Schematic diagram of an integrated TF current generator and FE-SEM image of ZnO nanorod arrays on a flexible ITO/PES substrate. Scale bar: 300 nm. b) Photographic image of the fully flexible charge-generating nanodevice. c) Photographic image of the bottom film (ZnO-nanorod arrays on the ITO/PES substrate) showing its high transparency.

[*] Dr. J.-Y. Choi, Dr. D. Choi, Dr. S. Y. Lee, Dr. J. M. Kim
Samsung Advanced Institute of Technology
Yongin, Gyeonggi, 446-712 (Republic of Korea)
E-mail: jaeyoung88.choi@samsung.com
Prof. S.-W. Kim, M.-Y. Choi, M.-J. Jin, Prof. I. Kim
Kumoh National Institute of Technology
School of Advanced Materials and System Engineering
Gumi, Gyeongbuk, 730-701 (Republic of Korea)
E-mail: kimsw@kumoh.ac.kr
Dr. S.-H. Kim
Electronics and Telecommunications Research Institute
IT Convergence Technology Research Division
Daejeon, 305-700 (Republic of Korea)

DOI: 10.1002/adma.200803605

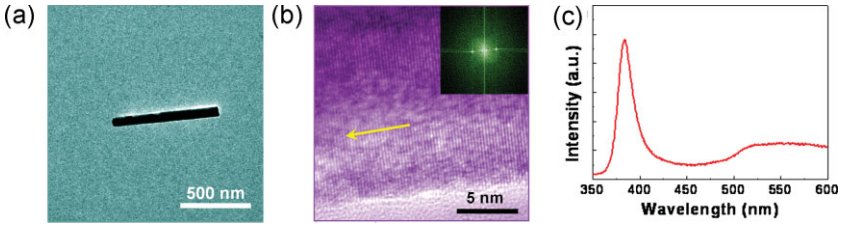

Figure 2. Structural and optical properties of ZnO nanorods grown on flexible ITO/PES substrates by the aqueous-solution method. a) Bright-field TEM image of a single ZnO nanorod. b) HRTEM image taken from the single ZnO nanorod. The inset is the FFT pattern of the HRTEM image. c) Room-temperature PL spectrum of the ZnO nanorods.

sulfone (PES) substrate. The top electrode was placed above the ZnO nanorod arrays. The integrated device was then sealed at the edges to prevent physical and chemical damage. Since the ZnO nanorods and the top electrode can be fabricated on flexible substrates, it is possible for the integrated nanodevice to be fully flexible (Fig. 1b). Furthermore, the device can be transparent, depending on the materials of the top electrode, since controlled ZnO-nanorod arrays are transparent (over 90%), as shown in Figure 1c. This device can itself generate a current via deformation of piezoelectric ZnO nanorods by external mechanical forces; this is the principle of the self-powered pressure sensor.

Figure 2a and b show transmission electron microscopy (TEM) images of a single ZnO nanorod (grown on the ITO/PES substrate) and the corresponding fast Fourier transformation (FFT) pattern taken from the nanorod shown in the high-resolution (HR) TEM image. The lattice distance based on lattice fringes along the growth direction of the ZnO nanorod is 0.52 nm, corresponding to the *c*-axis spacing of the (0002) atomic planes and showing the preferred growth direction as [0001]. Anisotropic growth of the ZnO crystal along the [0001] direction is due to the inherent polar properties of the material along the *c*-axis. FFT analysis of the ZnO nanorod indicates that the ZnO nanorods grown along the [0001] direction are predominantly single crystals. The mechanism of formation of the ZnO nanorods in aqueous solution has been described in detail in previous work.[11,16]

Figure 2c captures room-temperature photoluminescence (PL) of the ZnO nanorods on the ITO/PES substrate. The predominant peak around 383 nm is usually attributed to the recombination of free excitons (near band-edge emission). A broad deep-level emission band with a relatively weak emission intensity is also observed at about 550 nm. In general, broad deep-level emission prevails over free exciton-related emission in these solution-grown ZnO nanostructures.[16,17] It is well known that deep-level emission is mainly due to deep states in the band gap, which originate from defects such as zinc interstitials, oxygen vacancies, and their complexes in these nanostructures.[18] It may be concluded that the relatively weak deep-level emission from our ZnO nanorods is due to the formation of the small number of defects in the nanorods. Liu et al. suggested that an increased carrier density in ZnO nanowires speeds up the rate at which the piezoelectric charges are screened, whereas a very low carrier density prevents current flow through the ZnO nanowires and increases the inner and contact resistance of the nanowires.[19] The weak deep-level emission from the ZnO nanorods in this work therefore implies that they should be very effective in applications in charge-generating nanodevices, as a result of their density of point defects acting as carriers.

By controlling the seed layer density for the growth of ZnO nanorods, we can modulate the transparency of the resulting ZnO nanorod arrays. Figure 3 shows the transparency (approximately 70%) of an integrated nanodevice (nanodevice A). Since the transparency of an ITO/PES film for ZnO growth is about 82%, the transparency to visible light of the ZnO nanorod arrays can be estimated at about 92%, by considering the transparency of the ITO/PES top and bottom films. Transparency of ZnO nanorod arrays with random alignment and non-uniform distribution decreased to 15.7% (nanodevice B). We found that manipulation of the ZnO seed density is effective in controlling the alignment as well as the distribution of ZnO nanorods. ZnO seed nanoparicles with small diameters below 10 nm and uniform distribution lead to the formation of vertically aligned ZnO nanorods with uniform diameters during main growth. On the other hand, a nonuniform distribution of seed nanoparticles with larger diameters leads to seed agglomeration, resulting in the random alignment and nonuniform diameter distribution of ZnO nanorods.

Optimizing the seed density improved the vertical alignment and uniformity of the distribution of ZnO nanorods on ITO/PES films. The improved vertical alignment of the rods is one reason for the high transmittance obtained. Random orientation of nanorods would lead to strong Rayleigh scattering of light, which may occur when light passes through transparent solids. In view of the strong wavelength dependence ($\approx\lambda^{-4}$) of light scattering, blue light is scattered much more readily than red light. As shown in Figure 3, lower transmittance in the shorter-wavelength (blue) region in the ZnO nanorod sample, with a transparency of about 15% (nanodevice B), is consistent with Rayleigh scattering behavior. Also, the disorder in nanorod placement generally leads to strong suppression of transmission, as a result of plasmonic resonances related to the clustering of the nanorods.[20] Thus, it is apparent that the high transparency of the ZnO nanorods to

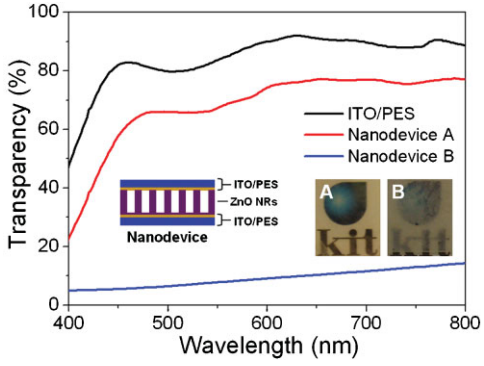

Figure 3. Transmittance spectra of charge-generating piezoelectric nanodevices with higher transparency (above 70%, indicated as "Nanodevice A") and much lower transparency (about 15%, indicated as "Nanodevice B") as well as the ITO-coated PES substrate. Inset images are photographs of the nanodevices (A and B: "Nanodevice A" and "Nanodevice B", respectively).

visible light (over 90%) is due to their good alignment and uniform distribution,[21] occurring even though they were grown on flexible ITO/PES films in aqueous solution at low temperature. Furthermore, it cannot be excluded that the high transparency of the ZnO nanorod arrays is due to the good crystallinity and low defect density of the nanorods consistent with the TEM and PL findings, since strain-induced point defects and impurities generally act as photon-scattering centers.

The Schottky contact between the ZnO nanorods and the top electrode is effective in generating high currents by means of the discharge of the carriers produced in bent ZnO nanorods.[1,14,19] To study current generation from fully flexible piezoelectric devices, we first applied PdAu as a top-electrode material, because Pd and Au have work functions greater than the electron affinity of n-type ZnO (naturally formed) for Schottky contact formation. In addition, since a zigzag or embossed structure of the top electrode has been shown to lead to high current generation,[1] 3D embossed PdAu convex arrays on a flexible PES substrate were prepared using a dimpled template, which had been fabricated by anodization and etching of aluminum (Fig. S2, Supporting Information). Each embossed PdAu specimen has a uniform diameter of about 100–150 nm and highly ordered convex arrays. A Ni film (thickness 500 nm) between the PdAu and the PES films was deposited using an electroplating method to avoid film cracking, and to maintain stable adhesion to the PES substrate. After the ZnO nanorod arrays and the embossed top electrode were integrated, we performed current–voltage measurements to confirm Schottky contact formation between the ZnO nanorod arrays and the top electrode (Fig. S3, Supporting Information).

We measured the current densities generated by the fully flexible piezoelectric nanodevice, with the top electrode consisting of embossed PdAu/Ni/PES (size $3 \times 3\,cm^2$), by applying forces to the top of the nanodevice (Fig. 4a). Currents were successfully detected, showing sensitive dependence on the external forces (0.3 kgf, 0.6 kgf, and 0.9 kgf). We chose the force range (<1 kgf load) by considering the force originating from the touch or slight push by a human finger (Fig. S4, Supporting Information). When the piezoelectric nanorods are deformed by mechanical forces, an electrical charge and a potential may be generated. We propose that current generation is due to the bending of slightly tilted ZnO nanorods and the direct compression of vertically aligned ZnO nanorods in the direction of the external pressures.

In the case of the bent nanorods (case I, Fig. 4c), charges are generated via the polarization created by ionic charges of lattice ions along the width. Unlike the vertically well-aligned nanorods, the tilted nanorods are easily bent with the application of mechanical force. The bending curvature of the tilted nanorod is proportional to the force applied to it. Since a positive potential is produced at the stretched side of the nanorod and a negative potential is induced at the compressed side, a larger applied force generates a larger piezoelectric potential difference across the nanorod. Based on previous reports, the maximum potential at the surface of the bent ZnO nanorod causing current generation can be specified as[22,23]

$$V_{max,s}^{\pm} \approx \pm 27(D/L)^3 y_m \quad (1)$$

where D and L denote the diameter and length of the nanorod, respectively, and y_m (nm) is the lateral displacement of the tip of the nanorod. This result shows that the potential generated is related to the aspect ratio of the nanorod rather than its dimensionality. If nanorods have a uniform aspect ratio, the piezoelectric potential is directly proportional to the maximum deflection at the tip. The piezoelectric potential generated is responsible for the piezoelectric current. However, when the embossed top electrode contacts the stretched surface of the nanorod or the central area of the nanorod top surface by applying a compressive force, little current flows across the interface (case II, Fig. 4c).

Furthermore, the charges in the direct compression of nanorods are generated by the electric polarization within ZnO nanorods along the length direction (case III, Fig. 4c). With force applied in the direction parallel to the vertically aligned ZnO nanorods, the centers of mass for positive and negative ions are shifted, resulting in a net dipole moment (polarization) along this direction. The potential generated by a piezoelectric material in this case is given by the standard formula $V = Fg_{33}L/A$, where F is the compressive force applied along the length of the nanorod, g_{33} is the potential output coefficient, L is the length of the vertically well-aligned nanorod, and A is the top surface area of the nanorod. The electric charge is estimated by $Q = CV$, where Q is the electric charge and C is the capacitance, given by $C = \varepsilon A/L$,

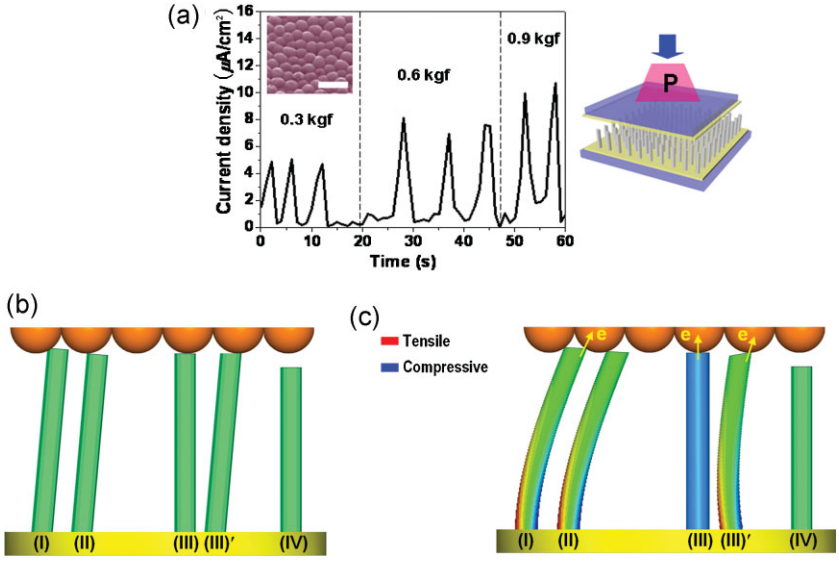

Figure 4. a) Current densities generated by the fully flexible piezoelectric nanodevice with size 3 cm × 3 cm (top electrode: 3D-shaped PdAu convex arrays on Ni/PES) as a function of the force applied to the top of the nanodevice, and a schematic image of the experiment to generate piezoelectric currents. Scale bar: 300 nm. b) and c) show schematic diagrams of four different types of nanorods before and after force application. Nanorods in cases I, III, and III' are active, and can generate output current. No current flows from the nanorod to the top electrode in the nanorods in cases II and IV.

where ε is the permittivity. Consequently, $Q = \varepsilon AV/L = \varepsilon g_{33}\ F = \varepsilon g_{33} AP$, where P is the pressure. This relation shows that the electric charge generated by applying pressure is proportional to the top surface area of the nanorod.[24] In this model of case III, we conclude that the larger diameter and the vertical alignment of piezoelectric nanorods lead to higher piezoelectric charge if the dramatic increase of the piezoelectric constant by 1D nanostructuring of ZnO[25] is neglected. We therefore believe that the high output-current density of 10 $\mu A\,cm^{-2}$, which we obtained from the device, is due to the combined effects of cases I and III above.

We also investigated the morphological effect of the top electrode by using a thin PdAu film with no corrugations (Fig. 5a). In case of flat thin top electrodes, the output current density fell to about 3.7 $\mu A\,cm^{-2}$ under a compressive force of 0.9 kgf, because current generation in the flat top electrode occurs mainly by the mechanism described for case III in Figure 4b and c. We expect the current-production mechanism of case I in Figure 4b and c to be ruled out in view of the geometrical alignment of the nanorods under the pushing mode, as shown in Figure 5b and c.

We also fabricated fully integrated TF piezoelectric current generators with ITO/PES top electrodes. Since the work function of ITO is lower than that of PdAu, Schotkky contact formation between ITO and ZnO nanorods is rather weak (Fig. S5, Supporting Information). As a result, the current density of $\approx$1 $\mu A\,cm^{-2}$ was lower than that from the current-generating device with the flat PdAu top electrode ($\approx$3.7 $\mu A\,cm^{-2}$). This current density is still adequate for use in force/pressure sensors. We further explored the durability of the integrated TF nanodevice. Both side surfaces of the device were observed by FE-SEM images after some dozens of tests had been performed. Figure 6b and c show the ITO surface and ZnO nanorod arrays,

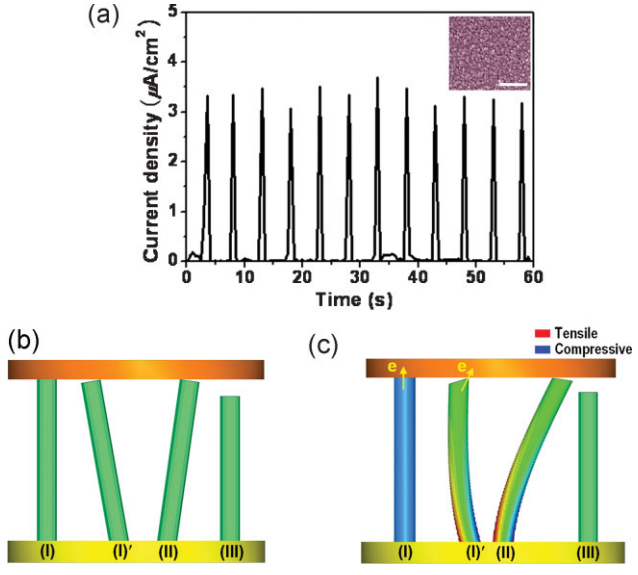

Figure 5. a) Current-density profile generated from the fully flexible piezoelectric nanodevice with a thin PdAu film with no corrugation (size 3 cm × 3 cm) under a periodically applied constant compressive force of 0.9 kgf. Scale bar: 300 nm. b) and c) show schematic diagrams of three different types of nanorods before and after application of a force. The nanorods in cases I and Í can generate output current, but no current flows from the nanorod to the top electrode in the nanorods in cases II and III.

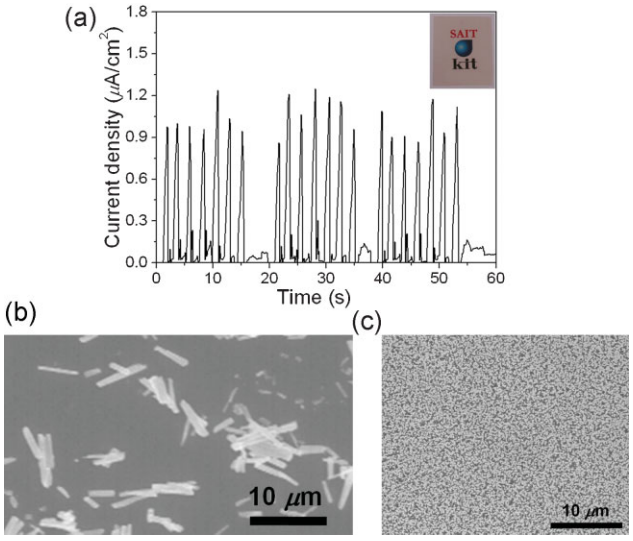

Figure 6. a) Current-density profile generated from the fully TF piezoelectric nanodevice with a flat ITO/PES top electrode (size 3 cm × 3 cm) under a periodically applied constant compressive force of 0.9 kgf. b) and c) are FE-SEM images showing the surfaces of the ITO and the ZnO-nanorod arrays, respectively, after some dozens of tests.

respectively, after testing. Although broken ZnO nanorods were found on the ITO surface, the fraction of broken nanorods is very small compared with the nanorods on the ZnO surface after testing. Since the ZnO nanorods were robust and stood up well on the ITO surface, the stress distribution on the ZnO nanorods (100 nm in diameter, and 1.5–2 μm long) under the maximum load of 0.9 kgf is not sufficient to fracture them (see Supporting Information, Fig. S6). This experiment therefore confirms that our TF piezoelectric nanodevice with ZnO nanorods can act as a reliable nanosystem device for applications such as touch sensors and artificial skins.

In summary, a mechanically powered integrated TF current generator with piezoelectric ZnO nanorods has been demonstrated. By controlling the transparency of the ZnO nanorod arrays, we developed fully transparent integrated nanodevices showing flexibility. The current density of the nanodevice was dependent on the morphology and the work function of the top electrode. A TF piezoelectric nanodevice with ITO/PES top electrode gave a current density of $\approx$1 $\mu A\,cm^{-2}$, which is sufficient for use as a force/pressure sensor. In view of the durability of our vertically grown ZnO-nanorod device, it has clear potential for use in electrical applications such as touch screens and tactile skin sensors.

Experimental

ZnO-Nanorod-Array Growth on ITO/PES Substrates: ZnO nanorods were synthesized using an aqueous-solution method and seed generation (see Supporting Information, Fig. S1). The ITO-film thickness was approximately 350 nm, and the sheet resistance was about 30 Ω/square. As a seed solution, we used zinc acetate dehydrate ($Zn(CH_3COO)_2{\cdot}2H_2O$, 0.01 M) dissolved in ethanol (100 mL) that had been heated at 90 °C. The seed solution was dropped onto the substrate and spin-coated at 1000 rpm for 60 s. The spin-coated substrate, covered with a ZnO-seed layer, was dried onto a hot template at 100 °C. ZnO nanorods were then formed in the

aqueous solution using zinc nitrate hexahydrate ($Zn(NO_3)_2 \cdot 6H_2O$, 0.025 M), hexamethylenetetramine (0.025 M), and deionized water (250 mL). Main growth of the ZnO nanorods was undertaken at 95 °C for 3 h.

Top-Electrode Fabrication: The detailed fabrication process of the top electrode with the embossed PdAu layer is presented in Figure S2 in the Supporting Information. First, an aluminum (Al)-coated Si wafer was anodized at 50 V for 10 min in oxalic acid for obtaining an anodic aluminum oxide (AAO) layer. The AAO layer formed was then removed, resulting in a dimpled Al surface. Second, a PdAu thin layer was deposited using ion sputtering on the dimpled template, and a Ni layer was subsequently deposited using an electroplating method onto the PdAu layer, to enhance adhesion between PdAu and PES. Finally, the Ni/PdAu double layer was taken off from the Al/Si template using physical attachment of a PES film.

Characterizations: FE-SEM was performed using a JEOL JSM 6500 instrument. HRTEM was carried out using a JEOL 2010F TEM (field emission) with an accelerating voltage of 200 kV. The 325 nm line of a He–Cd laser as an excitation source was used for PL measurements. Transmission spectra were obtained using a Varian Cary 5000 UV-Vis spectrometer. A Keithley 6485 Picoammeter was used for low-noise current measurements in order to detect currents generated by the flexible piezoelectric nanodevices. Current–voltage measurements to confirm Schottky-contact formation between the ZnO-nanorod arrays and the top electrode were carried out using an Agilent 4156A parameter analyzer.

Acknowledgements

M.-Y. C. and D. C. contributed equally to this work. The authors thank Dr. W.-M. Choi, S.-M. Yoon, H.-J. Shin, and Dr. E.-S. Kim for their helpful comments and experimental support. This work was financially supported by the Korea Research Foundation Grant funded by the Korean Government (MOEHRD, Basic Research Promotion Fund) (KRF-2008-331-D00294) and by Samsung Advanced Institute of Technology. Supporting Information is available online from Wiley InterScience or from the author.

Received: December 6, 2008
Revised: January 18, 2009
Published online: March 19, 2009

[1] X. D. Wang, J. H. Song, J. Liu, Z. L. Wang, *Science* **2007**, *316*, 102.
[2] X. D. Wang, J. Zhou, J. H. Song, J. Liu, N. S. Xu, Z. L. Wang, *Nano Lett.* **2006**, *6*, 2768.
[3] X. D. Wang, J. Liu, J. H. Song, Z. L. Wang, *Nano Lett.* **2007**, *7*, 2475.
[4] Z. L. Wang, *Adv. Funct. Mater.* **2008**, *18*, 1.
[5] Y. Qin, X. D. Wang, Z. L. Wang, *Nature* **2008**, *451*, 809.
[6] J. Zhou, Y. D. Gu, P. Fei, W. J. Mai, Y. F. Gao, R. S. Yang, G. Bao, Z. L. Wang, *Nano Lett.* **2008**, *8*, 3035.
[7] P. G. Gao, J. H. Song, J. Liu, Z. L. Wang, *Adv. Mater.* **2007**, *19*, 67.
[8] S. Xu, Y. Wei, J. Liu, R. Yang, Z. L. Wang, *Nano Lett.* **2008**, *8*, 4027.
[9] Y. F. Lin, J. H. Song, Y. Ding, S. Y. Liu, Z. L. Wang, *Appl. Phys. Lett.* **2008**, *92*, 022105.
[10] Y. F. Lin, J. Song, Y. Ding, S. Y. Lu, Z. L. Wang, *Adv. Mater.* **2008**, *20*, 3127.
[11] L. Vayssieres, K. Keis, S. Lindquist, A. Hagfelt, *J. Phys. Chem. B* **2001**, *105*, 3350.
[12] M. Law, L. E. Greene, J. C. Johnson, R. Saykally, P. Yang, *Nat. Mater.* **2005**, *4*, 255.
[13] J. Schrier, D. O. Demchenko, L. W. Wang, A. P. Alivisatos, *Nano Lett.* **2007**, *7*, 2377.
[14] Z. L. Wang, J. H. Song, *Science* **2006**, *312*, 242.
[15] R. Yang, Y. Qin, L. Dai, Z. L. Wang, *Nat. Nanotechnol.* **2009**, *4*, 34.
[16] D.-H. Kim, S.-D. Lee, K.-K. Kim, G.-S. Park, J.-M. Lee, S.-W. Kim, *J. Nanosci. Nanotechnol.* **2008**, *8*, 4688.
[17] L. E. Greene, M. Law, J. Goldberger, F. Kim, J. C. Johnson, Y. Zhang, R. J. Saykally, P. Yang, *Angew. Chem. Int. Ed.* **2003**, *42*, 3031.
[18] D. Li, Y. H. Leung, A. B. Djurisic, Z. T. Liu, M. H. Xie, S. L. Shi, S. J. Xu, W. K. Chan, *Appl. Phys. Lett.* **2004**, *85*, 1601.
[19] J. Liu, P. Fei, J. H. Song, X. D. Wang, C. S. Lao, R. Tummala, Z. L. Wang, *Nano Lett.* **2008**, *8*, 328.
[20] A. I. Rahachou, I. V. Zozoulenko, *J. Opt. A* **2007**, *9*, 265.
[21] S. P. Anthony, J. I. Lee, J. K. Kim, *Appl. Phys. Lett.* **2007**, *90*, 103107.
[22] Y. F. Gao, Z. L. Wang, *Nano Lett.* **2007**, *7*, 2499.
[23] J. Song, X. Wang, J. Liu, H. Liu, Y. Li, Z. L. Wang, *Nano Lett.* **2008**, *8*, 203.
[24] M. Akiyama, Y. Morofuji, T. Kamohara, K. Nishikubo, M. Tsubai, O. Fukuda, N. Ueno, *J. Appl. Phys.* **2006**, *100*, 114318.
[25] R. Zhu, D. Wang, S. Xiang, Z. Zhou, X. Ye, *Nanotechnology* **2008**, *19*, 285712.